M-PAM Joint Optimal Waveform Design for Multiuser VLC Systems Over ISI Channels

Jie Lian, Mohammad Noshad, and Maïté Brandt-Pearce, *Senior Member, IEEE*

***Abstract*—Visible light communication is a candidate technique to provide high-speed data transmissions. This paper proposes a joint optimal waveform design algorithm for visible light communication systems using M-ary pulse amplitude modulation to support multiple users. Transmitted waveforms and minimum mean squared error filters are jointly optimized to minimize the intersymbol and multiple access interferences. Based on different channel conditions, the designed waveforms and modulation constellation sizes can be adaptively adjusted to guarantee the highest bit rates. Channel uncertainty is also considered in this paper. Compared with optical code division multiple access and time division multiple access, the algorithm proposed can provide higher bit rates. In addition, the proposed algorithm can flexibly adjust the illumination level by changing the optimization constraints. An offline waveform design algorithm is then proposed to diminish the optimization computation time. A waveform lookup table can be established offline in advance, and the proper waveforms can be selected from the table based on the actual channel gains in real time. The performance of the offline algorithm can be estimated by using the channel uncertainty model.**

***Index Terms*—Dimming control, equalization, intersymbol interference, joint optimization, M-PAM, multiple access interference, offline design, precoding, visible light communications, waveform design.**

I. Introduction

With the rapid development of wireless applications, conventional radio frequency (RF) communications cannot meet the increasing requirements of high-speed wireless data transmission [1]. The congested RF spectrum and regulated RF band usage limit the development of RF communications. Therefore, an alternative wireless high-speed communications method is needed. Visible light communications (VLC) is a promising solution to provide high-speed wireless data transmission [2], [3]. Light emitting diodes (LEDs) that work as transmitters in VLC systems have many advantages, such as simple modulation, high power efficiency (dual system: illumination and communication) and high security. This paper proposes a high-speed multiuser VLC system that can be used to augment or replace the downlink portion of a Wi-Fi system.

Intersymbol interference (ISI) is one of the biggest challenges for high-speed data transmissions. The slow rise-time of lighting LEDs and multi-path propagation are two factors leading to ISI. For indoor VLC systems, multi-path propagation comes from reflections of the light from the ceiling, walls, furniture and other reflective surfaces and limits systems operating at bandwidth above 100 MHz [4]. The 3 dB modulation bandwidth of commercial lighting LEDs is limited to a few tens of MHz [5]. Thus, the bandlimited LED is the dominant factor to introduce ISI.

Equalization that can be realized by either hardware or software is an attractive solution to mitigate ISI and obtain a high data rate. Some researchers have proposed a pre-equalization circuit to increase the data rate and have achieved up to 340 Mb/s transmission using on-off keying (OOK) with a bit error rate (BER) of 2×10^{-3} [6]. Using red-green-blue LEDs and a hardware equalization circuit, Gb/s data rate can be achieved [5]. As for software equalizers, the zero forcing (ZF) algorithm is a popular signal processing method to mitigate the effects of ISI in RF communications [7], [8]. ZF has also been applied in optical wireless communications [9]. A least mean squared error equalizer using a training sequence for indoor VLC systems was proposed in [10], and both linear and decision feedback equalizers were discussed.

A high bandwidth efficiency modulation, such as M-ary pulse amplitude modulation (M-PAM) is a good choice to provide a high-speed connection for VLC systems since the light emitted from the LEDs is non-coherent, and intensity modulation should be used. Using M-PAM, a $(\log_2 M)$-fold increase in the data rate compared to OOK can be achieved. Recently, an adaptive M-PAM scheme was proposed to provide a higher data rate for multiuser VLC systems [11]–[15]. Instead, orthogonal frequency division multiplexing (OFDM) can be used to increase the data rate while combating ISI [16], [17]. However, optical OFDM systems experience a relatively high peak to average power ratio (PAPR) that can result in a severe nonlinear distortion of the transmitted signals because of the LED peak transmitted power constraint. Researchers have shown that M-PAM with equalization can provide better performance than OFDM for VLC systems [13], [18].

Another important research topic in indoor VLC is how to choose a multiple access technique. Multiple access interference (MAI) can be a factor limiting the throughput of multiuser systems. Time division multiple access (TDMA) is one approach

Manuscript received September 30, 2017; revised April 4, 2018 and May 26, 2018; accepted May 27, 2018. Date of publication June 11, 2018; date of current version June 29, 2018. This work was supported by the National Science Foundation (NSF) through the STTR program under award number 1521387. *(Corresponding author: Maïté Brandt-Pearce.)*

J. Lian and M. Brandt-Pearce are with the Charles L. Brown Department of Electrical and Computer Engineering, University of Virginia, Charlottesville, VA 22904 USA (e-mail: jl5qn@virginia.edu; mb-p@virginia.edu).

M. Noshad is with VLNcomm, Charlottesville, VA 22911 USA (e-mail: noshad@vlncomm.com).

Color versions of one or more of the figures in this paper are available online at http://ieeexplore.ieee.org.

Digital Object Identifier 10.1109/JLT.2018.2846187

that can be used due to its small operational complexity [19], [20]. A space division multiple access (SDMA) technique using angular diversity of the transmitters to support and separate multiple users in indoor VLC environments was proposed in [21], but the bandlimited characteristic of the LEDs was not considered. Recently, we proposed an optical code division multiple access (OCDMA) indoor VLC system using a resource allocation algorithm to support multiple users and reduce the MAI [22].

In this paper, both problems, high-speed transmission and multiple access, are solved by using a joint optimal waveform (JOW) design algorithm for multiple input single output (MISO) multiuser systems. The authors recently proposed a waveform design algorithm in [23], yet MAI was not considered. In the current paper, this idea is expanded to design waveforms capable of reducing both ISI and MAI. In this system, unique waveform designs and minimum mean squared squared error (MMSE) filters for different users are optimized jointly. In addition, to achieve a high data rate, an M-PAM modulation scheme is applied.

In this work, the proposed JOWs have two functions: separating users and reducing ISI. Similar to OCDMA, the proposed JOWs are discrete time sequences that are unique to users. But superior to OCDMA, JOWs combat ISI and MAI simultaneously, and can be adaptively redesigned when the channel state changes. The JOWs can be optimized for different transmitted symbol rates by maximizing the signal to interference plus noise ratio (SINR). For a fixed required bit error rate (BER), by changing the JOW and M-ary modulation constellation size, the maximum data rate can be found. The JOWs can be designed to allow dimming of the light by changing the illumination level, determined by the average waveform power. However, the illumination level is difficult to change in OCDMA or TDMA. Shadowing and light reflection from surrounding moving objects can cause channel estimation errors, which add uncertainty to the channel state information (CSI). In this paper, the uncertainty is taken into account by modeling the assumed channel impulse response error as an additive Gaussian random process [24], [25].

To address the real-time computational complexity of performing the requisite optimization, an off-line waveform design algorithm using a pre-established waveform table is then proposed. In practice, the proper waveforms can be selected from the table based on the actual channel gains. The performance of the off-line algorithm can be estimated by using the channel uncertainty model.

The remainder of the paper is organized as follows. The indoor channel model is described in Section II. In Section III, the M-PAM joint optimal waveform design algorithm is derived. Numerical results are discussed in Section IV. The paper is concluded in Section V.

II. Channel Model

In a typical indoor VLC system, LEDs are used to transmit data and illuminate the indoor area at the same time. Since the light from the LEDs is non-coherent, intensity modulation and direct detection (IM/DD) are employed. Considering the multipath propagation in the indoor channel and bandwidth limit of the LEDs, the optical link can experience severe ISI.

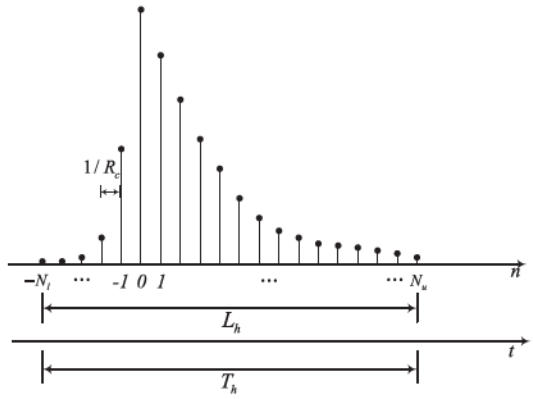

Fig. 1. Discrete time version of a truncated LED response.

In this paper, we assume there are Q LED lamps and K users with one photodetector (PD) per user receiving signals, and each lamp serves to transmit downlink signals to all the users. In this work, the bandwidth of the indoor channel is limited by the LED rise time [26]. Therefore, the overall channel impulse response from LED q to user k can be modeled as

$$h_{qk}(t) = g_{qk} h_l(t), \quad \begin{matrix} q = 1, \ldots, Q \\ k = 1, \ldots, K \end{matrix} \tag{1}$$

where $h_l(t)$ is the impulse response of the LEDs, which can be modeled as a lowpass filter. The impulse response of all LEDs is assumed to be the same. g_{qk} is the LOS channel gain from LED q to user k, which can be calculated as in [27, Eq. (1)]. $\mathbf{h}_{qk} = (h_{qk}[1], h_{qk}[2], \ldots, h_{qk}[L_h])^T$ represents the discrete time version of the truncated channel impulse response from LED q to user k.

Fig. 1 shows an example of a truncated channel impulse response that lasts T_h seconds. T_c represents the sampling period, which can be represented as $T_c = 1/R_c$, where R_c is the sampling rate. The length of the discrete time truncated channel impulse response can be calculated as $L_h = T_h/T_c$.

In this paper, the channel impulse response with uncertainty from LED q to user k is modeled as

$$\mathbf{h}^*_{qk} = \mathbf{h}_{qk} + \Delta\mathbf{h}_{qk}, \tag{2}$$

where $\Delta\mathbf{h}_{qk} = (\Delta h_{qk}[1], \Delta h_{qk}[2], \ldots, \Delta h_{qk}[L_h])^T$ is the uncertainty in modeling the channel impulse response. As often done in literature [24], [25], the elements in $\Delta\mathbf{h}_{qk}$ are assumed to be independent of each other and modeled as Gaussian random variables with zero mean and variance σ_h^2.

Since lighting LEDs used in this paper are narrow bandwidth devices, for a small indoor space the time difference between the signal received by different LEDs is short compared to the dispersive LED response, and can be neglected. For a larger room, the channel gains from the farther LEDs are weaker than that of the closer ones. The average magnitude error between the actual impulse response and the model in (1) is less than 6% for our simulation scenario. In this paper we assume the channel model is as in (1) and include such errors as channel uncertainty according to (2).

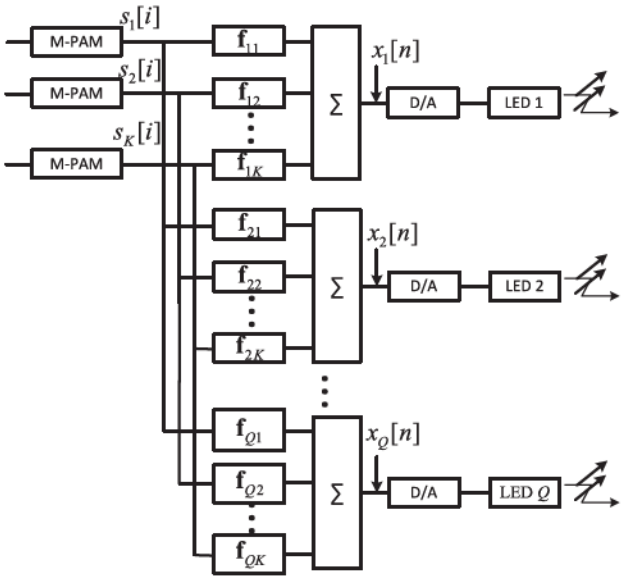

Fig. 2. Block diagram of the transmitters for the proposed M-PAM joint optimal waveform design system.

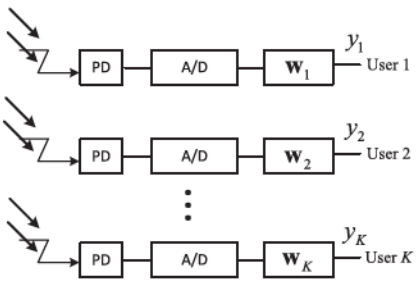

Fig. 3. Block diagram of the proposed receiver.

III. M-PAM Joint Optimal Waveform Design

A. Transmitted and Received Signals

A block diagram of the proposed M-PAM joint optimal waveform design system is shown in Fig. 2. The designed transmitted waveform and MMSE filter for different users are jointly optimized. After M-PAM modulation, the M-ary amplitude symbol stream for user k at time instant i can be represented as $s_k[i] \in \{0, \frac{1}{M_k-1}, \frac{2}{M_k-1}, \ldots, 1\}$, and each symbol carries $\log_2 M_k$ bits, where M_k is the modulation constellation size for user k. $s_k[i]$ is assumed to be uniformly distributed. After the waveform design, the transmitted sequence from LED q can be represented as

$$x_q[m] = \sum_{k=1}^{K} \sum_{i=-\infty}^{\infty} s_k[i] f_{qk}[m - iL_f], \tag{3}$$

where $\mathbf{f}_{qk} = (f_{qk}[1], f_{qk}[2], \ldots, f_{qk}[L_f])^T$ is the designed waveform for LED q and user k. L_f is the number of samples used to represent the waveform. The channel gain from each LED to each user could be different, and the waveform for each LED and user is unique.

As shown in Fig. 3, after low pass filtering and sampling at the receiver using sampling rate R_c, the received signal for user k can be represented as

$$r_k[m] = \sum_{q=1}^{Q} \sum_{j=-\infty}^{\infty} x_q[m+j] h_{qk}[-j] + n_k[m]. \tag{4}$$

After applying the MMSE filter, the received signal for user k can be written in matrix form as

$$y_k[i] = \mathbf{w}_k^T \sum_{q=1}^{Q} \mathbf{H}_{qk} \mathbf{x}_q + \mathbf{w}_k^T \mathbf{n}_k + b_k, \tag{5}$$

where the MMSE filter for user k is represented by $\mathbf{w}_k = (w_k[1], w_k[2], \ldots, w_k[L_w])^T$ with length L_w. b_k is a constant needed for the MMSE estimator due to the nonzero mean of the transmitted signals [28]. $\mathbf{n}_k = (n_k[1], n_k[2], \ldots, n_k[L_w])^T$ is the additive Gaussian noise for user k with zero mean and variance $\sigma_n^2 = N_0 R_c$, where N_0 is the noise spectral density. $\mathbf{H}_{qk}$ is a Toeplitz matrix that can be represented as

$$\mathbf{H}_{qk} = \left(S_L(\mathbf{h}_{qk}, \frac{L_w - 1}{2}), \ldots, \mathbf{h}_{qk}, \ldots, S_R(\mathbf{h}_{qk}, \frac{L_w - 1}{2}) \right)^T, \tag{6}$$

where $S_L(\mathbf{x}, m)$ and $S_R(\mathbf{x}, m)$ are two functions that operate as m circular shifts on $\mathbf{x}$, to the left and right, respectively.

The vector of transmitted samples that affect $y_k[m]$ is denoted $\mathbf{x}_q = (x_q[-N_u], \ldots, x_q[0], \ldots, x_q[N_l])^T$. $N_l + N_u + 1 = L_h$, where L_h describes the length of successive samples that overlap and cause ISI. N_l and N_u represent past and future samples that contribute to ISI, respectively as shown in Fig. 1. From (3), the mth element of the vector $\mathbf{x}_q$ can be calculated as $\sum_k s_k[\lfloor m/L_f \rfloor] f_{qk}[\mathrm{mod}(m, L_f)]$, where $\lfloor m/L_f \rfloor$ represents the largest integer less than m/L_f, which is the number of successive M-PAM data that overlap causing ISI, and $\mathrm{mod}(m, L_f)$ is the remainder of $\lfloor m/L_f \rfloor$.

B. Waveform Design Algorithm with Imperfect CSI

For the JOW algorithm proposed in this paper, the CSI must be known at the transmitters. However, in practice, CSI cannot be estimated perfectly. To account for the imperfect CSI, the imperfect channel model $\mathbf{h}_{qk}^*$ is substituted for $\mathbf{h}_{qk}$ in (5). The received signal for user k after the MMSE filter with channel uncertainty can be represented as

$$y_k[i] = \mathbf{w}_k^T \sum_{q=1}^{Q} (\mathbf{H}_{qk} + \Delta\mathbf{H}_{qk}) \mathbf{x}_q + \mathbf{w}_k^T \mathbf{n}_k + b_k, \tag{7}$$

which consists of four parts: the target (intended data) for user k, the uncertainty caused by the imperfect CSI, the ISI plus MAI, and the noise. $\Delta\mathbf{H}_{qk}$ represents the additive channel uncertainty matrix, which can be obtained by

$$\Delta\mathbf{H}_{qk} = \left(S_L\left(\Delta\mathbf{h}_{qk}, \frac{L_u 1}{2}\right), \ldots, \Delta\mathbf{h}_{qk}, \ldots, S_R\left(\Delta\mathbf{h}_{qk}, \frac{L_w - 1}{2}\right) \right)^T. \tag{8}$$

The MMSE filter for each user can be obtained using simple signal manipulation, as shown in the appendix. Using this receiver filter given in (27), the signal to interference plus noise

ratio (SINR) for user k can be calculated as in [29],

$$\mathrm{SINR}_k = \frac{\text{Signal}}{\text{Uncertainty} + \text{ISI} + \text{MAI} + \text{Noise}}, \tag{9}$$

where

$$\text{Signal} = \frac{2M_k - 1}{6M_k - 6}$$

$$\text{Uncertainty} = \sigma_h^2 \mathbf{w}_k^T \sum_{q=1}^{Q}\sum_{p=1}^{Q} \mathbf{\Sigma}_{qp}\mathbf{w}_k, \tag{10}$$

$$\text{Noise} = \sigma_n^2 \mathbf{w}_k^T \mathbf{w}_k, \tag{11}$$

$$\begin{aligned}\text{ISI} + \text{MAI} = {} & \mathbf{w}_k^T \sum_{q=1}^{Q}\sum_{p=1}^{Q} \mathbf{H}_{qk}\mathbf{\Sigma}_{qp}\mathbf{H}_{pk}^T\mathbf{w}_k \\ & - 2\mathbf{w}_k^T \sum_{q=1}^{Q} \mathbf{H}_{qk}\mathbf{e}_q + \frac{2M_k - 1}{6M_k - 6} \\ & - 2b_k \mathbf{w}_k^T \sum_{q=1}^{Q} \mathbf{H}_{qk}\mathbf{m}_q - b_k + b_k^2,\end{aligned} \tag{12}$$

where $\mathbf{\Sigma}_{qp}$, $\mathbf{e}_q$ and $\mathbf{m}_q$ are also given in the appendix.

From (9), $\mathbf{F} = (\mathbf{F}_1, \mathbf{F}_2, \ldots, \mathbf{F}_Q)$, $\mathbf{M}$=$(M_1, M_2, \ldots, M_K)$ and R_c are the only variables needed to find the SINR_k, where $\mathbf{F}_q = (\mathbf{f}_{q1}, \mathbf{f}_{q2}, \ldots, \mathbf{f}_{qK})$. We denote $\mathrm{SINR}_k = \gamma_k(\mathbf{F}, \mathbf{M}, R_c)$. Then, for M-PAM modulation, the BER for user k can be approximated by [30]

$$\mathrm{BER_k} \approx \frac{M_k - 1}{M_k \log_2 M_k} \mathrm{erfc}\left(\sqrt{\frac{\gamma_k(\mathbf{F}, \mathbf{M}, R_c)}{(M_k - 1)^2}}\right), \tag{13}$$

where $\mathrm{erfc}(\cdot)$ is the complementary error function, which is defined as $\mathrm{erfc}(x) = \frac{2}{\sqrt{\pi}} \int_x^\infty e^{-u^2}\,\mathrm{d}u$.

For different data rates, the waveform design algorithm can adaptively adjust the waveforms for each user to minimize the ISI. For a fixed data rate and modulation constellation size, the optimal waveforms can be obtained by maximizing the minimum SINR of all the users, through which each user can achieve a fair performance. The optimization cost function is

$$\mathbf{F}^* = \arg\max_{\mathbf{F}} \min_k \gamma_k(\mathbf{F}, \mathbf{M}, R_c), \tag{14}$$

where $\mathbf{F}^*$ is the optimal value for $\mathbf{F}$. When optimizing the waveforms, a peak transmitted power constraint must be considered, which can be represented as

$$\forall\ i,\ k \text{ and } q, \sum_{k=1}^{K} f_{qk}[i] \le P^{\max},\ \text{and}\ f_{qk}[i] \ge 0, \tag{15}$$

where $P^{\max}$ represents the peak LED transmitted power. After the optimization process (finding the optimal waveforms in (14)), the SINR for all the users is similar.

The transmitted data rate for user k can be calculated as

$$R_b^{(k)} = R_c(\log_2 M_k)/L_f, \tag{16}$$

where the sampling rate, R_c, for each user is assumed to be the same. R_c/L_f represents the transmitted symbol rate. The maximum data rate for each user is constrained by the required BER, $B^{\max}$, since the communication quality needs to be taken into account. For a fixed SINR, the modulation constellation size determines the BER and the transmitted data rate. Therefore, to maximize the data rate for each user, the following problem needs to be solved:

$$\begin{aligned} & M_k^* = \max\ M_k,\ \forall\ k = 1, \ldots, K \\ & \text{s.t.}\ \frac{M_k - 1}{M_k \log_2 M_k} \mathrm{erfc}\left(\sqrt{\frac{\gamma_k(\mathbf{F}^*, \mathbf{M}, R_c)}{(M_k - 1)^2}}\right) < B^{\max}, \end{aligned} \tag{17}$$

where M_k^* is the optimal value for M_k to maximize the throughput for user k.

The steps for solving (17) and getting the optimal waveforms are described in Algorithm 1. The genetic algorithm (GA), which is a powerful heuristic searching method, is used for finding the optimal waveforms [31].

Algorithm 1: Optimal waveforms and the highest data rate.

```
Initialize: R_c, L_f;
repeat
  for (Each user, k) do
    while (Increase modulation size M_k) do
      while (Constraint in (17) is satisfied) do
        Genetic Algorithm
          Initialization for GA;
          Generate random waveforms as individuals (1st Gen);
          repeat
            Evaluate the SINR, γ_k(F, M, R_b);
            Select the candidate waveforms by checking constraint (15);
            Match, mutate and crossover;
            Generate the next generation of waveforms;
          until γ_k converges;
          Get F*, solution to (14);
        Calculate BER using (13);
        Calculate R_b^(k) using (16);
      end
    end
  end
  Increase R_c;
until R_b^(k) converges;
Output: The maximum R_b^(k), optimal M, and F*
```

C. Illumination and Dimming Control

For VLC systems, illumination control is an important consideration. The transmitted optical power can provide wireless access as well as illumination. The maximum illumination level in the room depends on the peak transmitted power and the illumination potential, defined as the ratio of the average transmitted power to the peak LED power. For this work, the illumination potential using JOW can be represented as

$$\eta_J = \frac{1}{2QKL_f P^{\max}} \sum_{q=1}^{Q}\sum_{k=1}^{K}\sum_{l=1}^{L_f} f_{qk}[l]. \tag{18}$$

The coefficient $1/2$ comes from the uniform distribution of $s_k[i]$.

In the optimization process, η_J can be used as an optimization constraint and adjusted to satisfy the specific illumination requirements by changing the values of waveforms. The illumination level can be controlled by finding the optimal waveform as shown in Algorithm 1, inserting (18) as an additional constraint.

For OCDMA, the illumination potential is fixed, and depends on the codewords. The illumination potential using optical orthogonal codes (OOC) as waveforms in an OCDMA system can be calculated as

$$\eta_C = \begin{cases} W/2L_c, & K \leq W \\ K/2L_c, & K > W \end{cases}, \tag{19}$$

where W is the weight for the OCDMA codeword, and L_c is the length of the code. Therefore, if a certain OCDMA code is selected, for a certain number of active users, the illumination potential of using OCDMA cannot be changed. JOW has a more flexible illumination potential than OCDMA due to the optimally designed waveforms. When using the proposed JOW algorithm in indoor VLC systems, the illumination level can be adjusted by designing for a specific illumination potential.

For TDMA, only one user is served per time slot, and the data for each user can be sent directly. Barring any DC offset, the illumination potential for TDMA is a constant, which can be represented as $\eta_T = 1/2$. Compared with JOW, we can state that TDMA is at least as power efficient as JOW, i.e., $\eta_J \leq \eta_T$.

D. Off-Line Waveform Design

The proposed waveform design algorithm is a time consuming process due to the non-linear and non-convex optimization. In this section, we propose an off-line solution to make the system adapt in real-time. In the off-line method, the waveforms for multiple users are calculated in advance. Given the number of lamps in the space, tables of the waveforms for different numbers of users and channel gains can be created. In typical VLC systems, only a few users can be served by any one lamp. In practice, depending on the number of users and the channel gains, the proper waveforms for the users can be selected from the pre-established tables.

Since we assume than the LED impulse response, $h_l(t)$, can be estimated perfectly, the only factors that can affect the off-line solution's performance are the channel gains. The more channel gain choices that are used to create the table, the better the performance the off-line waveforms algorithm can achieve. One table is created for each possible value of K. The candidate channel gains that are used to create the table can be represented as a matrix

$$\mathbf{U}_K = \begin{pmatrix} \mu_{11} & \mu_{12} & \cdots & \mu_{1K} \\ \mu_{21} & \mu_{22} & \cdots & \mu_{2K} \\ \vdots & \vdots & \ddots & \vdots \\ \mu_{L_T 1} & \mu_{L_T 2} & \cdots & \mu_{L_T K} \end{pmatrix}, \tag{20}$$

where each row represents one set of candidate channel gains for the K users in the table. L_T is the number of sets of channel gains, which decides the size of the table. To create the table, μ_{ik} can be used to replace g_{qk}, $\forall\, q$ in (1). Then, the waveform lookup table can be created by using the proposed algorithm in this paper.

TABLE I
PARAMETERS USED FOR SMALL INDOOR ENVIRONMENT

Size of the small room	5 m × 5 m × 3 m
Number of LEDs, Q	4
Locations of the lamps (m)	(1.25, 1.25, 3), (1.25, 3.75, 3) (3.75, 1.25, 3), (3.75, 3.75, 3)
Locations of the users (m)	(1.0, 2.2, 0.8), (1.5, 1.5, 0.8) (2.5, 3.4, 0.8), (4.3, 2.5, 0.8) (4.0, 2.1, 0.8), (3.3, 2.6, 0.8) (2.2, 1.8, 0.8)
Responsivity	0.5 A/W
Area of the photodetector	0.01 cm^2
Radiated optical power per lamp	3 W
LED semiangle	60^o
Noise spectral density	1×10^{-9} mW/Hz
3 dB bandwidth of LEDs	20 MHz
Modulation constellation size	2, 4, 8, 16
BER requirement, $B^{\max}$	10^{-4}

During operation, the table corresponding to the number of active users K is first selected. Then, based on the real estimated channel gains for the multiple users, the proper waveforms can be selected by using the following criterion

$$i_q^* = \arg\min_i \sum_{k=1}^{K} (\mu_{ik} - g_{qk})^2, \ \forall\, q, \tag{21}$$

where i_q^* is the index of the channel gains selected for LED q. The performance of the off-line algorithm is essentially equivalent to a channel uncertainty with

$$\sigma_h^2 = \frac{1}{K} \sum_{k=1}^{K} (\mu_{i^* k} - g_{qk})^2. \tag{22}$$

IV. NUMERICAL RESULTS AND DISCUSSIONS

In this section, numerical results of the performance of the proposed system are shown. Unless otherwise noted, the parameters used to obtain the numerical results are shown in Table I. The locations of the users in Table I are randomly chosen, the channel gains of which are computed using [27, Eq. (1)], using the parameters shown in Table I. The parameters used in this paper, such as the room dimension and locations of the LEDs, are typical for indoor spaces, and often used as a benchmark scenario in VLC research literature [2], [4], [32]. For the genetic algorithm, 50 random initial individuals and up to 100 generations are used for the optimization.

A. Perfect CSI

In this paper, adaptive M-PAM is used together with JOW to enhance the transmitted data rate. Only 2, 4, 8, and 16-PAM are considered in this work for our numerical results. The number of samples per waveform, L_f, is an adjustable parameter, which needs to be sufficiently large to reduce the ISI and MAI. Fig. 4 shows numerical results of the optimized data rate with different numbers of samples per waveform to satisfy a BER $= 10^{-4}$ using M-PAM. The three users are located according to the first

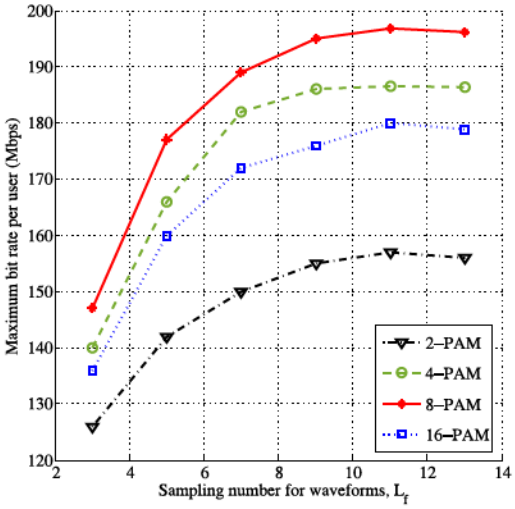

Fig. 4. Transmitted data rate for different numbers of samples per waveform for 3 users, with no η_J constraint.

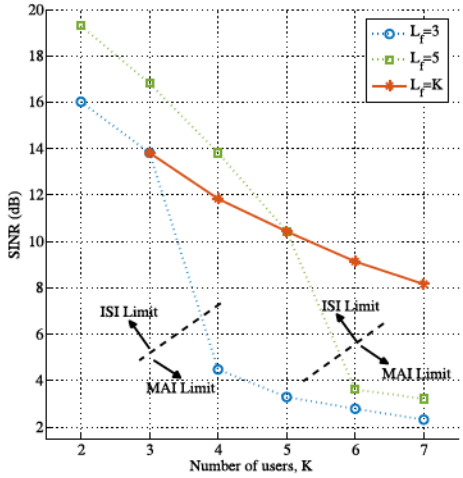

Fig. 5. SINR for different users using 8-PAM, with no η_J constraint.

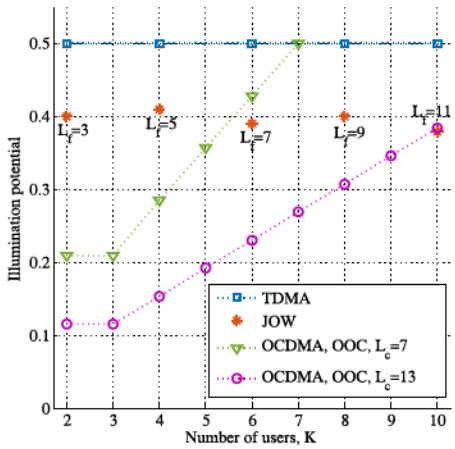

Fig. 6. Illumination potential for different numbers of users.

three entries of Table I. In general, as the number of samples per waveform increases, a higher data rate can be supported by using M-PAM. In this figure, the bit rate plateaus, as the ability of the algorithm to reduce ISI and MAI by using waveforms and MMSE filters is limited by the LED bandwidth, i.e., more samples would not add more information. Thus, considering the computational cost and design complexity, the optimal number of samples per waveform is 11 for this case. For LEDs with a different bandwidth, the optimal number of samples per waveform may vary.

From the results in Fig. 4, 8-PAM can provide the highest data rate compared to the other modulation schemes. Since there is a BER constraint guaranteeing the communications quality, a larger modulation constellation would require a higher SINR. When the system cannot provide a high enough SINR to satisfy the BER requirement, a lower level modulation needs to be used or the symbol rate needs to be reduced. For 16-PAM to satisfy the BER requirement, the transmitted symbol rate is sacrificed so that the bit rate is lower than for 8-PAM. We envision an adaptive procedure that adjusts the constellation size depending on the channel quality and received SINR.

More users can introduce more MAI. Fig. 5 shows the SINR for up to 7 users. The channel gains for these 7 users are calculated by using the parameters shown in Table I. If the number of users K exceeds the number of samples per waveform L_f, the MAI dominates over the ISI. In Fig. 5 the numerical results show that the SINR drops sharply when K is larger than L_f, and the system enters the MAI limited region. For example, when $L_f = 3$, the degrees of freedom in the waveform design per user is 3, which is enough for three users but not more. Depending on the number of active users in this room, we can select $L_f = K$ samples per waveform, maintaining an acceptable performance as the number of users increases, as shown in the figure. This flexibility and high SINR comes at the cost of increased computation.

The illumination potential is shown in Fig. 6. From the result, TDMA has the highest illumination potential since it only serves one user per time slot. The illumination potential using TDMA is the expected value of the data, which is the maximum achievable. OCDMA and JOW follow a similar principle to support multiple users. Depending on the codewords or waveforms, the power efficiencies for illumination of OCDMA and JOW are different. For OCDMA, this illumination potential increases as the number of users increases. Eventually, when the number of active users is equal to the length of the selected OCDMA code, the illumination potential for OCDMA can reach its maximum value since the value of the sum of the unmodulated codewords is $P^{\max}$. In Fig. 6, when the number of users is lower than 7, a OOC code with length $L_c = 7$ is enough. However, when the number of users is greater than 7, a length $L_c = 13$ OOC code is needed, since the length 7 OOC code cannot support that many users. A longer code length has a lower illumination potential for OCDMA. Comparing OCDMA and JOW, JOW can provide higher illumination potentials for most cases, and the illumination potential of JOW can achieve 80% of the maximum value for the parameters considered.

Fig. 7 shows numerical results of SINR for JOW, OCDMA and TDMA techniques. The first 3 users in Table I are used. In this result, η_J is added to Algorithm 1 as an optimization constraint for JOW. For OCDMA and TDMA, η_C and η_T are fixed. For both OCDMA and TDMA, MMSE filters are applied

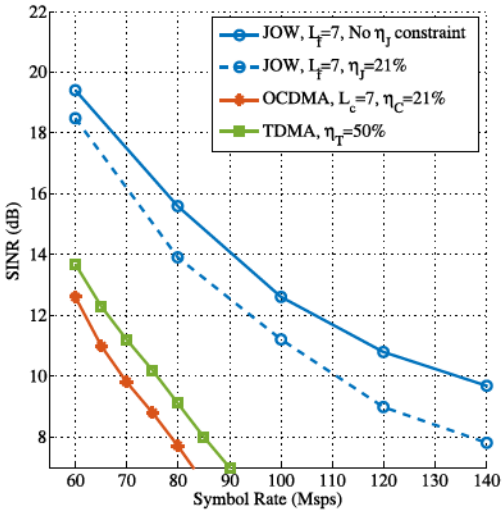

Fig. 7. SINR comparison of JOW, OCDMA and TDMA for 3 users using 8-PAM. Peak power is fixed.

TABLE II
MAXIMUM DATA RATES USING M-PAM AVERAGED OVER 3 USERS, PARAMETERS FROM TABLE I

Data rate (Mbps)	2-PAM	4-PAM	8-PAM	16-PAM
No ISI, ideal channel	532	476	403	352
JOW, $L_f = 7$	151	180	189	172
OCDMA, $L_c = 7$	78	121	137	164
No-equalization	24	44	61	69

at the receivers. For the same transmitted symbol rate, JOW has a higher SINR than TDMA and OCDMA since the optimized waveforms can reduce ISI and MAI together with the MMSE filter. Since there is no MAI for TDMA, the SINR for TDMA is higher than OCDMA. When the JOW has the same illumination potential as OCDMA, the SINR for JOW is greater than for OCDMA.

Since a higher modulation level requires a higher SINR to satisfy the communication quality (BER requirement), a larger modulation constellation size cannot always provide a higher data transmission rate. In Table II, numerical results for the maximum data rate with different modulation constellation sizes are shown using the parameters in Table I. 2-PAM can provide the highest data rate for the ideal channel. Since there is no ISI for the ideal channel (MAI without ISI), using a higher level modulation does not increase the throughput. For the case where the LED bandlimit is applied but no equalization is used, a higher level modulation can provide a higher transmission data rate. With the help of JOW, ISI can be reduced; therefore, the optimal modulation constellation size for JOW is 8 for this case. OCDMA has more ISI than JOW, thus 16-PAM needs to be used for OCDMA to achieve the maximum data rate. In general, as the ISI increases, the optimal modulation constellation size increases.

B. Imperfect CSI

Numerical results for the imperfect CSI case are given in this section. To describe the impact of the channel uncertainty, a normalized error, normalized to the squared average channel gain, is defined as

$$\beta_h = \frac{\sigma_h^2}{\left(\frac{1}{QK}\sum_{k=1}^{K}\sum_{q=1}^{Q} g_{qk}\right)^2}. \tag{23}$$

β_h captures the magnitude of the channel uncertainty with respect to the channel gains.

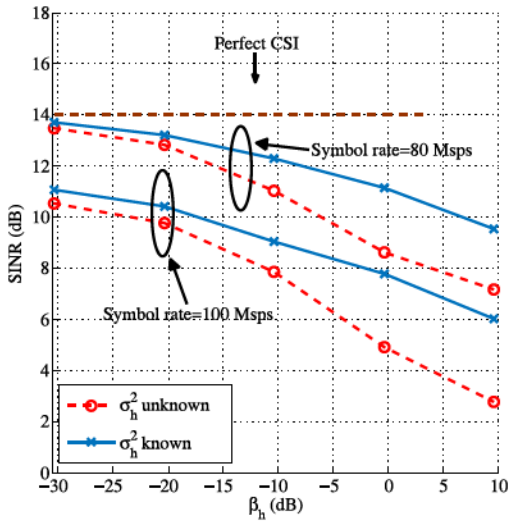

Fig. 8. SINR for imperfect CSI with different uncertainty variance using 8-PAM, $L_f = 7$ and 3 users. $\eta_J = 21\%$.

Fig. 8 shows a comparison of the perfect and imperfect CSI cases. For the imperfect CSI case, if the channel uncertainty is known and when β_h defined in (23) is 10 dB, then there is about a 4 dB SINR penalty compared with the perfect CSI case.

In Fig. 8, numerical results also show cases with and without knowing the channel uncertainty information, i.e., the uncertainty variance, σ_h^2. From the results, the algorithm that knows σ_h^2 can obtain a higher SINR than if it does not know the variance. When $\beta_h = 10$ dB, knowing the variance can provide about 2 dB SINR advantage over not knowing the variance.

The same method used to estimate the effect of imperfect CSI can be used to evaluate the off-line algorithm. The difference between g_{qk} and μ_{ik} can be regarded as a known channel uncertainty. From this results, if $\beta_h = 10$ dB, the performance of the off-line algorithm can provide about 4 dB less SINR compared to the regular (on-line) algorithm.

C. Computational Cost Discussions

A comparison of the computational cost between the on-line and off-line algorithms is presented in this section. For the on-line JOW, the computational cost is determined by the number of variables that need to be optimized, which is $K \times L_f \times Q$. As discussed above, L_f should be at least as large as the number of total active users. Typical numbers for a small room would be 3 users with 4 LED lamps, and if we choose $L_f = 11$, there are 132 variables that need to be solved. Using the genetic algorithm with 50 initial individuals and 50 generations, the time consumption is approximately 10^5 seconds by using a GA solver in MATLAB running on a PC with an Intel i5 processor and a 2G memory.

For the off-line JOW, a lookup table needs to be established in advance. Before looking up the waveform parameters, a proper table should be selected based on the number of users. We assume that the computational cost for looking up the waveform parameters in the table can be neglected. Therefore, the storage space for this lookup table is the only cost that needs to be taken into account. Without any loss of generality, if we use 8 bits for quantization, the case of $K = 3$, $L_f = 11$, and $Q = 4$ needs only about 0.13 KB per candidate channel gain without using any compression techniques. The more candidate channel gains in the table, the better the performance of the off-line JOW can achieve. For example, if the number of candidate channel gains, $L_T = 1000$, only about 0.13 MB storage is used. Therefore, only a small storage space is needed for a well-established lookup table.

For a large room with a large number of active users and LED lamps, the indoor area can be divided into small cells based on the positions of users and lamps [22]. In this case, both the on-line and off-line JOW can be applied.

V. Conclusion and Future Work

In this paper, we propose a joint optimal waveform design algorithm using an adaptive M-PAM modulation scheme to provide high data transmission rates for multiple users. In this algorithm, the transmitted waveforms from each LED lamp to each user are uniquely designed to reduce the ISI and MAI. Unlike TDMA and OCDMA, the waveforms for JOW can be designed as pre-equalizers and used to separate users. The waveforms are optimized together with the MMSE filters at the receiver to provide maximum data rates, which are higher than OCDMA or TDMA. Using JOW the modulation constellation size can be adaptively adjusted under different SINR conditions and BER requirements. For a three users case, the maximum achievable bit rate per user is 196 Mbps using the parameters given in this paper.

The illumination level can be easily adjusted in JOW by setting an illumination potential constraint when optimizing the waveforms. Since the waveforms can be adaptively adjusted—they are fixed in OCDMA and TDMA—dimming control for JOW is more flexible than OCDMA or TDMA.

In this work, channel uncertainty and imperfect CSI cases are discussed. In practical scenarios, the performance of JOW depends on the accuracy of the channel gain estimates; the channel uncertainty model proposed in this paper gives an estimate of the performance penalty. From the numerical results, the algorithm that knows the channel uncertainty variance, σ_h^2, can achieve a higher SINR than if it does not know σ_h^2.

Since the on-line JOW is time consuming to derive, an off-line waveform design solution is proposed. The performance of the off-line solution can be estimated as if it were a channel uncertainty. For the off-line JOW, the time cost for table lookup is negligible, and only a small amount of memory is required.

In future work, hardware experiments based on an FPGA implementation will be developed for validation to simulation results. The experimental performance is expected to be better than the analytical results since the channel uncertainty is likely to be correlated, which should result in lower error compared to the independent sample-to-sample error assumed in this paper. We plan to benchmark our experimental results as compared with other modulation and multiple-access techniques. Mobility of users will also be explored in future work. Tracking techniques can be used to predict the channel gains that will allow JOW to design waveforms in advance.

Appendix

This appendix describes the derivation of the MMSE filters considering the channel uncertainty. The mean-squared error, J_k, for user k is defined as

$$J_k = E_{\mathrm{s,n},\Delta\mathrm{h}}\{(y_k[i] - s_k[i])^2\}, \tag{24}$$

where $E_{\mathrm{s,n},\Delta\mathrm{h}}\{\cdot\}$ represents expectation with respect to the transmitted symbols $(s_1, s_2, \ldots, s_K)$, the noise and the channel uncertainty, which are statistically independent. Substituting (7) into (24), we obtain

$$\begin{aligned} J_k = {} & \mathbf{w}_k^T \sum_{q=1}^{Q}\sum_{p=1}^{Q} \mathbf{H}_{qk}\boldsymbol{\Sigma}^{(qp)}\mathbf{H}_{pk}^T\mathbf{w}_k \\ & + \sigma_h^2 \mathbf{w}_k^T \sum_{q=1}^{Q}\sum_{p=1}^{Q} \boldsymbol{\Sigma}^{(qp)}\mathbf{w}_k \\ & - 2\mathbf{w}_k^T \sum_{q=1}^{Q} \mathbf{H}_{qk}\mathbf{e}_q + \sigma_n^2 \mathbf{w}_k^T\mathbf{w}_k + \frac{2M_k - 1}{6M_k - 6} \\ & - 2b_k \mathbf{w}_k^T \sum_{q=1}^{Q} \mathbf{H}_{qk}\mathbf{m}_q - b_k + b_k^2, \end{aligned} \tag{25}$$

where $\boldsymbol{\Sigma}^{(qp)} = E_{\mathrm{s}}\{\mathbf{x}_q\mathbf{x}_p^T\}$. The (m,n)th element of $\boldsymbol{\Sigma}^{(qp)}$ can be calculated as

$$\sigma_{mn}^{(qp)} = \begin{cases} \sum_{k=1}^{K} \frac{2M_k-1}{6M_k-6} f_{qk}[u] f_{pk}[v] \\ \quad + \frac{1}{4}\sum_{k\neq z}\sum_{z\neq k} f_{qk}[u] f_{pz}[v], & i = j, \\ \frac{1}{4}\sum_{k=1}^{K}\sum_{z=1}^{K} f_{qk}[u] f_{pz}[v], & i \neq j \end{cases} \tag{26}$$

where $i = \lfloor m/L_f \rfloor$ and $j = \lfloor n/L_f \rfloor$; $u = \mathrm{mod}(m, L_f)$ and $v = \mathrm{mod}(n, L_f)$. $\mathbf{e}_q = E_{\mathrm{s}}\{s_k[i]\cdot\mathbf{x}_q\}$ and $\mathbf{m}_q = E_{\mathrm{s}}\{\mathbf{x}_q\}$.

Solving for $\frac{\partial J_k}{\partial b_k} = 0$ and $\frac{\partial J_k}{\partial \mathbf{w}_k} = 0$, the MMSE filter for user k can be obtained as

$$\begin{aligned} \mathbf{w}_k &= \left(\mathbf{T}_k + \sigma_n^2\mathbf{I}\right)^{-1} \sum_{q=1}^{Q} \mathbf{H}_{qk}\mathbf{e}_q \\ b_k &= \frac{1}{2} - \mathbf{w}_k^T \sum_{q=1}^{Q} \mathbf{H}_{qk}\mathbf{m}_q, \end{aligned} \tag{27}$$

where

$$\mathbf{T}_k = \sum_{q=1}^{Q}\sum_{p=1}^{Q} \mathbf{H}_{qk}\boldsymbol{\Sigma}^{(qp)}\mathbf{H}_{pk}^T + \sigma_h^2\mathbf{w}_k^T \sum_{q=1}^{Q}\sum_{p=1}^{Q} \boldsymbol{\Sigma}^{(qp)}, \tag{28}$$

and $\mathbf{I}$ is the identity matrix.

REFERENCES

[1] A. Jovicic, J. Li, and T. Richardson, "Visible light communication: Opportunities, challenges and the path to market," *IEEE Commun. Mag.*, vol. 51, no. 12, pp. 26–32, Dec. 2013.

[2] T. Komine and M. Nakagawa, "Fundamental analysis for visible-light communication system using LED lights," *IEEE Trans. Consum. Electron.*, vol. 50, no. 1, pp. 100–107, Feb. 2004.

[3] H. Haas, L. Yin, Y. Wang, and C. Chen, "What is LiFi?" *J. Lightw. Technol.*, vol. 34, no. 6, pp. 1533–1544, Mar. 2016.

[4] K. Lee, H. Park, and J. R. Barry, "Indoor channel characteristics for visible light communications," *IEEE Commun. Lett.*, vol. 15, no. 2, pp. 217–219, Feb. 2011.

[5] X. Huang, J. Shi, J. Li, Y. Wang, and N. Chi, "A Gb/s VLC transmission using hardware preequalization circuit," *IEEE Photon. Technol. Lett.*, vol. 27, no. 18, pp. 1915–1918, Sep. 2015.

[6] Y. Wang, L. Tao, Y. Wang, and N. Chi, "High speed WDM VLC system based on multi-band CAP64 with weighted pre-equalization and modified CMMA based post-equalization," *IEEE Commun. Lett.*, vol. 18, no. 10, pp. 1719–1722, Oct. 2014.

[7] A. Schmidt, R. Schober, and W. Gerstacker, "Single-carrier frequency-division multiple access transmission with physical layer network coding over ISI channels," in *Proc. 21st Eur. Wireless Conf.*, May 2015, pp. 1–7.

[8] S. H. Song and K. B. Letaief, "Diversity analysis for linear equalizers over ISI channels," *IEEE Trans. Commun.*, vol. 59, no. 9, pp. 2414–2423, Sep. 2011.

[9] D. Lee and J. Kahn, "Coding and equalization for PPM on wireless infrared channels," in *Proc. IEEE Global Commun. Conf.*, 1998, pp. 201–206.

[10] T. Komine, J. Lee, S. Haruyama, and M. Nakagawa, "Adaptive equalization system for visible light wireless communication utilizing multiple white LED lighting equipment," *IEEE Trans. Wireless Commun.*, vol. 8, no. 6, pp. 2892–2900, Jun. 2009.

[11] M. Zhang *et al.*, "4.05-gb/s RGB LED-based VLC system utilizing PS-manchester coded nyquist PAM-8 modulation and hybrid time-frequency domain equalization," in *Proc. Opt. Fiber Commun. Conf. Exhib.*, Mar. 2017, pp. 1–3.

[12] P. Haigh, Z. Ghassemlooy, S. Rajbhandari, I. Papakonstantinou, and W. Popoola, "Visible light communications: 170 Mb/s using an artificial neural network equalizer in a low bandwidth white light configuration," *J. Lightw. Technol.*, vol. 32, no. 9, pp. 1807–1813, May 2014.

[13] D. J. F. Barros, S. K. Wilson, and J. M. Kahn, "Comparison of orthogonal frequency-division multiplexing and pulse-amplitude modulation in indoor optical wireless links," *IEEE Trans. Commun.*, vol. 60, no. 1, pp. 153–163, Jan. 2012.

[14] J. Du, W. Xu, H. Zhang, and C. Zhao, "Visible light communications using spatial summing PAM with LED array," in *Proc. IEEE Wireless Commun. Netw. Conf.*, Mar. 2017, pp. 1–6.

[15] J. Lian and M. Brandt-Pearce, "Adaptive M-PAM for multiuser MISO indoor VLC systems," in *Proc. IEEE Global Commun. Conf.*, 2016, pp. 1–7.

[16] A. Azhar, T. Tran, and D. O'Brien, "A Gigabit/s indoor wireless transmission using MIMO-OFDM visible-light communications," *IEEE Photon. Technol. Lett.*, vol. 25, no. 2, pp. 171–174, Jan. 2013.

[17] H. Elgala, R. Mesleh, and H. Haas, "Indoor optical wireless communication: Potential and state-of-the-art," *IEEE Commun. Mag.*, vol. 49, no. 9, pp. 56–62, Sep. 2011.

[18] J. Lian, M. Noshad, and M. Brandt-Pearce, "Comparison of DCO-OFDM and M-PAM for LED-based communication system," arXiv:1806.06420 [cs.IT], Jun. 2018.

[19] J. M. Luna-Rivera, R. Perez-Jimenez, J. A. Rabadan-Borjes, J. F. Rufo-Torres, V. Guerra, and C. Suarez-Rodriguez, "Multiuser scheme for indoor visible light communications using RGB LEDs," in *Proc. Int. Work Conf. Bio-Inspired Intel.*, 2014, pp. 119–123.

[20] M. Biagi, A. M. Vegni, and T. D. C. Little, "LAT indoor MIMO-VLC-localize, access and transmit," in *Proc. Int. Workshop Opt. Wireless Commun.*, 2012, pp. 1–3.

[21] Z. Chen and H. Haas, "Space division multiple access in visible light communications," in *Proc. IEEE Int. Conf. Commun.*, 2015, pp. 5115–5119.

[22] J. Lian and M. Brandt-Pearce, "Multiuser MIMO indoor visible light communication system using spatial multiplexing," *J. Lightw. Technol.*, vol. 35, no. 23, pp. 5024–5033, Dec. 2017.

[23] J. Lian and M. Brandt-Pearce, "Joint optimal waveform design for multiuser VLC systems over ISI channel," in *Proc. IEEE Int. Conf. Commun.*, 2017, pp. 1–7.

[24] K. Ying, H. Qian, R. J. Baxley, and S. Yao, "Joint optimization of precoder and equalizer in MIMO VLC systems," *IEEE J. Sel. Areas Commun.*, vol. 33, no. 9, pp. 1949–1958, Sep. 2015.

[25] K. H. Park, Y. C. Ko, and M. S. Alouini, "On the power and offset allocation for rate adaptation of spatial multiplexing in optical wireless MIMO channels," *IEEE Trans. Commun.*, vol. 61, no. 4, pp. 1535–1543, Apr. 2013.

[26] L. Zeng *et al.*, "Equalisation for high-speed visible light communications using white-LEDs," in *Proc. Int. Symp. Commun. Syst., Netw. Digit. Signal Process.*, Jul. 2008, pp. 170–173.

[27] J. Lian, M. Noshad, and M. Brandt-Pearce, "Multiuser MISO indoor visible light communications (invited paper)," in *Proc. Asilomar Conf. Signals, Syst. Comput.*, 2014, pp. 1729–1733.

[28] S. Haykin, *Adaptive Filter Theory*, 4th ed. Englewood Cliffs, NJ, USA: Prentice-Hall, 2001.

[29] J. G. Proakis, *Digital Communications*, 5th ed. New York, NY, USA: McGraw-Hill, 2008.

[30] Z. Ghassemlooy, W. Popoola, and Rajbhandari,*Optical Wireless Communications: System and Channel Modeling with MATLAB*. Boca Raton, FL, USA: CRC Press, 2013.

[31] K. Deb, A. Pratap, S. Agarwal, and T. Meyarivan, "A fast and elitist multiobjective genetic algorithm: NSGA-II," *IEEE Trans. Evol. Comput.*, vol. 6, no. 2, pp. 182–197, Apr. 2002.

[32] M. Noshad and M. Brandt-Pearce, "Hadamard-coded modulation for visible light communications," *IEEE Trans. Commun.*, vol. 64, no. 3, pp. 1167–1175, Mar. 2016.

Jie Lian received the Ph.D. degree in electrical engineering from the University of Virginia, Charlottesville, VA, USA, in 2017. He is a currently a Research Associate with the University of Virginia. His current research interests include signal processing, wireless communications, and visible light communications.

Mohammad Noshad received the Ph.D. degree in electrical engineering from the University of Virginia, Charlottesville, VA, USA, in 2013. He was a postdoctoral researcher with Harvard University from 2014 to 2016. He is a co-founder of VLNComm, Charlottesville, VA, USA, a pioneer in developing LiFi technology. His research interests include visible light communications, free-space optical communications, information and coding theory, and statistical machine learning.

Dr. Noshad was the recipient of many awards for his work on LiFi systems, including the Best Paper Award at the IEEE Global Communications Conference in 2012. He was a technical program committee member in various IEEE conferences and workshops.

Maïté Brandt-Pearce (SM'99) is a Professor of electrical and computer engineering and Executive Associate Dean for Academic Affairs of the School of Engineering and Applied Science, University of Virginia, Charlottesville, VA, USA. She joined UVA after receiving the Ph.D. degree in electrical engineering from Rice University in 1993. She has more than two hundred technical publications. Her research interests include nonlinear effects in fiber-optics, free-space optical communications, visible light communications, cross-layer design of optical networks subject to physical layer degradations, body area networks, and radar signal processing.

Dr. Brandt-Pearce is the recipient of an NSF CAREER Award and an NSF RIA. She is a co-recipient of Best Paper Awards at ICC 2006 and IEEE Global Communications Conference 2012. She had served on the editorial board of IEEE TRANSACTION OF COMMUNICATIONS, IEEE COMMUNICATIONS LETTERS, and the IEEE/OSA Journal of Optical Communications and Networks and Springer Photonic Network Communications. She was Jubilee Professor with Chalmers University, Sweden, in 2014. After serving as General Chair of the Asilomar Conference on Signals, Systems and Computers in 2009, she was a Technical Vice-Chair of IEEE Global Communications Conference 2016. She is a member of Tau Beta Pi and Eta Kappa Nu. She co-edited a book entitled *Cross-Layer Design in Optical Networks*, Springer Optical Networks Series, 2013.